Eur Biophys J (1988) 16:219–229

European Biophysics Journal

Proton transfer reactions in aqueous solutions of pyridoxamine phosphate

J. Reiter [1], P. Schuster [1]*, H. Winkler [2], and F. Eggers

[1] Institut für Theoretische Chemie und Strahlenchemie der Universität Wien, Währingerstrasse 17, A-1090 Wien, Austria
[2] Max-Planck-Institut für Biophysikalische Chemie, Postfach 2841, D-3400 Göttingen, Federal Republic of Germany

Received March 2, 1988/Accepted in revised form June 10, 1988

Abstract. UV-visible and ^{13}C NMR measurements described in the literature and our ^{31}P NMR measurements support the following mechanism of proton transfer reactions in aqueous solutions of pyridoxamine phosphate: Only the tautomeric equilibrium between neutral form, $\mathbf{A}_N$, and zwitterion, $\mathbf{A}_Z$, which is analogous to the tautomeric equilibrium of 3-hydroxypyridine in aqueous solution, is important, and that equilibrium does not change upon the dissociation of the second phosphate proton. With these simplifying assumptions, we have simulated the relaxation spectrum of the proton transfer reactions of pyridoxamine phosphate in water using parameters from analogous reactions and compared it with our ultrasound and temperature jump measurements. We have found that the relaxation process measured by the temperature jump experiment is mainly caused by the overall reaction $\mathbf{A}_N = \mathbf{A}_Z$ (or $\mathbf{A}_N^- = \mathbf{A}_Z^-$) and the ultrasound absorption at the isoelectric point between pK_2 and pK_3 is mainly caused by the overall reaction $\mathbf{A}^+ + x\,\mathbf{A}_N^- + (1-x)\,\mathbf{A}_Z^- = y\,\mathbf{A}_N + (2-y)\,\mathbf{A}_Z$, $0 \leqq x \leqq 1$, $0 \leqq y \leqq 2$.

Key words: Relaxation kinetics, ultrasound absorption, temperature jump, proton transfer, vitamin B 6

Introduction

Proton transfer reactions of dibasic acids in aqueous solution have been extensively investigated (Schuster et al. 1976, 1977; Dubois and Dreyfus 1978; Yiv et al. 1978; Reiter et al. 1988). In most systems, the equilibration between neutral form and zwitterion, $\mathbf{A}_N = \mathbf{A}_Z$, is the dominant reaction near the isoelectric point. The overall reaction $\mathbf{A}^+ + \mathbf{A}^- = x\,\mathbf{A}_N + (2-x)\,\mathbf{A}_Z$, $0 \leqq x \leqq 2$, may also be observed at the isoelectric point if the pK values of the dibasic acid are not too far apart. In addition, the proton dissociation reactions of the cation and the protonation reactions of the anion, or the corresponding hydrolysis reactions, are important near the pK values.

Intermolecular proton transfer in water is well understood (Eigen 1963). In particular, it has been found that intermolecular proton transfers from and to oxygen and nitrogen atoms are usually diffusion controlled and that their rate constants in the thermodynamically favored direction may be estimated with the Debye-Smoluchowski equation. Intramolecular proton transfer in water, however, is less well understood. For 3-hydroxypyridine, a simple analog of pyridoxamine phosphate, no evidence has been found for this reaction (Schuster et al. 1976). It is believed that the reactive groups of the dibasic acid have to be close together. Dubois and Dreyfus (1978) have investigated a number of dibasic acids; only for 6-chloro-2-hydroxypyridine did they find an intramolecular proton transfer reaction with a rate constant of $2 \cdot 10^4\ s^{-1}$. For o-amino-benzoic acid an intramolecular transfer rate of $9 \cdot 10^6\ s^{-1}$ has been determined (Reiter et al. 1988).

Pyridoxamine phosphate (PAMP) belongs to the class of vitamin B 6 compounds. Pyridoxal phosphate, a close derivative, is the coenzyme of glycogen phosphorylase and it is believed that the vitamin B 6 compound serves as an intramolecular proton transfer catalyst (Feldmann et al. 1975). The environment in the enzyme is, of course, different from water which might change the probability of intramolecular proton transfer dramatically. For instance, intramolecular proton

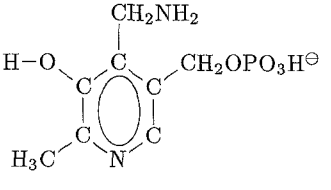

PAMP

* To whom offprint requests should be sent

transfer in methanol is usually much faster than in water. 3-hydroxypyridine shares two functional groups with vitamin B 6 compounds, but no proton transfer has been found for it, vide supra. We wanted to test whether additional functional groups, which are present in pyridoxamine phosphate compared with 3-hydroxypyridine, might alter the probability of that reaction.

Pyridoxamine phosphate is a pentabasic acid. Consequently, the mechanism of proton transfer reactions, is exceedingly complicated. However, experience has shown that the rate constants of the intermolecular proton transfer reactions in the thermodynamically favored direction can be estimated from the Debye-Smoluchowski eqution. In addition, near equilibrium the kinetics can be described by independent normal reactions, which facilitates the analysis. In this work, we study the kinetics of pyridoxamine phosphate in aqueous solution with the ultrasound and the temperature jump method and compare the results with the simulated relaxation spectrum.

Experiments and methods

^{31}P *NMR measurements*

The spectra were measured on a Bruker 270 MHz NMR spectrometer with phosphoric acid as external standard at a concentration of pyridoxamine phosphate of 0.1 mol l^{-1} in water. Since we added NaOH solution to adjust, the pH, the sample was slightly diluted during the titration.

Simulation of relaxation spectra and relaxation kinetics

The fundamental reference is Eigen and DeMaeyer (1974). See also Bernasconi (1986) for general information and Reiter et al. (1988) for additional references.

Ultrasound experiments

The ultrasound experiments were done as described in the literature (Eggers 1967/1968; Eggers and Funck 1973).

Temperature jump measurements

The measurements were done with the cable temperature jump apparatus built G. Hoffmann in Göttingen (Hoffmann 1972; Pörschke 1976). The sample was prepared in a 0.5 *M* KCl solution. Since the pH of the highly diluted solutions varied with time, we used the following procedure. The sample was freshly prepared and its pH was measured. Then it was degased, brought into the apparatus and thermostated for 5 min. After the measurement, the pH was determined again. If the two measured pH values were different, we used the average. We made only one temperature jump experiment per sample because pyridoxamine phosphate undergoes slow photolytic decomposition (Reiber 1972). The absorption at 330 nm was monitored during the experiment.

Proton transfer equilibria of pyridoxamine phosphate

Since pyridoxamine phosphate is a pentabasic acid, there exist, at least in principle, 24 differently protonated species in aqueous solution: the ion $\mathbf{A}^{2+}$, four forms of $\mathbf{A}^{+}$, seven forms of the overall neutral species $\mathbf{A}$, seven forms of $\mathbf{A}^{-}$, four forms of $\mathbf{A}^{2-}$ and the ion $\mathbf{A}^{3-}$. 23 equilibrium constants need to be known to calculate all equilibrium concentrations. Of those, only the five overall dissociation constants and one tautomeric constant are determined, see Table 1 and below. Fortunately, many of the 24 possible species occur in very small concentrations and can be neglected. The mechanism shown in Fig. 1 is in agreement with the available data. We first describe this mechanism and then discuss its validity. It is usually assumed that a phosphate proton dissociates first from $\mathbf{A}^{2+}$. The second proton dissociates from either the nitrogen in the aromatic ring or from the phenolic hydroxy group. The resulting equilibrium of neutral form, $\mathbf{A}_N$, and zwitterion, $\mathbf{A}_Z$, is analogous to that of 3-hydroxypyridine. The third proton is assumed to dissociate from the phosphate group, giving rise to an equilibrium between negatively charged ions $\mathbf{A}_N^-$ and $\mathbf{A}_Z^-$. Later in the text, we will refer to them also as neutral form and zwitterion. The fourth proton dissociates from either the nitrogen in the aromatic ring, or from the phenolic hydroxy group, yielding $\mathbf{A}^{2-}$. This step is analogous to the second dissociation step of 3-hydroxypyridine. The last proton dissociates from the amino group.

The five overall pK values have been determined by titration (Williams and Neilands 1954). Metzler et al. (1973) and Morozov et al. (1966) measured the equilibrium constants with UV-visible spectroscopy. With this technique, only three of the constants can be determined since the dissociation of phosphate protons does not change the absorption spectrum (Morozov et al. 1966). In addition to the three dissociation constants, Metzler et al. determined also the tautomeric equilibrium constant $K_T = \mathbf{A}_Z/\mathbf{A}_N = 9.3$. They arrived at that value by assuming that the ratio of the peak areas of neutral form and zwitterion is similar to that of 3-hydroxypyridine. They specified only one value for K_T, i.e., they seemingly assumed that there is no difference between K_T and K_T^-, where K_T^- is the tautomeric equilibrium constant for $\mathbf{A}_N^-$ and $\mathbf{A}_Z^-$. However, Metzler et al. (1973) mentioned also the possibility that at the pK_2 the amino proton could already

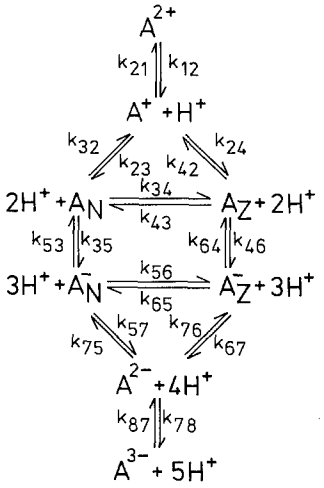

Fig. 1. Protolysis reactions and intramolecular proton transfer reaction of pyridoxamine phosphate

Table 1. Equilibrium constants of pyridoxamine phosphate

	a	b	c	d	e
pK_1	2.5				
pK_2	3.69	3.36	3.12		
pK_3	5.76				5.71
pK_4	8.61	8.46	8.33		
pK_5	10.92	10.67	10.4	~11	
K_T		9.3			

a: Titration (Williams and Neilands 1954); *b*: UV-visible spectroscopy (Metzler et al. 1973); *c*: UV-visible spectroscopy (Morozov et al. 1966); *d*: ^{13}C NMR (Jaworsky and O'Leary 1979); *e*: ^{31}P NMR, this work

dissociate to some extent, yielding a mixture of three isomers. Morozov et al. (1966) did not consider tautomeric equilibria and measured only three overall dissociation equilibrium constants. They noted, however, that the absorption spectrum does not change with the dissociation of the third proton, i.e., phosphate proton. This observation supports the hypothesis that the dissociation of the second phosphate proton does not change the tautomeric equilibrium. From investigations with ^{13}C NMR (Jaworsky and O'Leary 1979) it can be concluded that the phenolic proton dissociates predominantly at pK_2, that the proton from the nitrogen in the ring dissociates predominantly at pK_4 and that the proton from the amino group dissociates predominantly at pK_5. These observations are in agreement with a K_T much larger than unity and support the mechanism given in Fig. 1.

Andersen and Martell (1964) have investigated the equilibria of the related compound pyridoxal phosphate with IR spectroscopy. They concluded that at the pK_2 the proton dissociated either from the phosphate group or from the ring nitrogen, yielding a different tautomeric equilibrium than the one considered

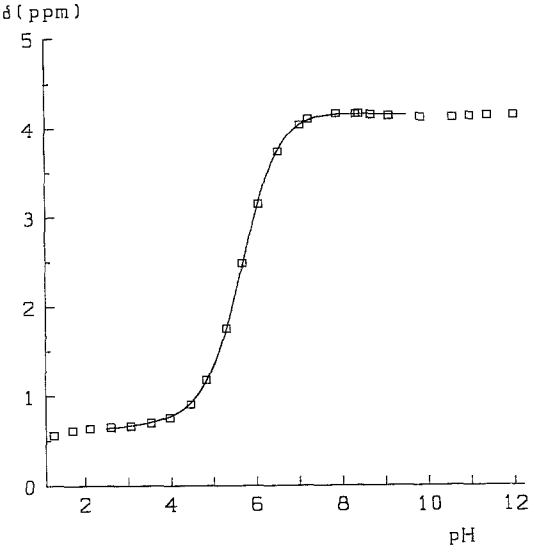

Fig. 2. ^{31}P NMR data of pyridoxamine phosphate. For the fit, the chemical shifts of the once negatively charged phosphate group and the twice negatively charged phosphate group were taken to depend linearly on pH, i.e., $\delta^- = \delta_1^- + \delta_2^-$ pH and $\delta^{2-} = \delta_1^{2-} + \delta_2^{2-}$ pH. The chemical shifts δ (*squares*) between pH 2.2 and pH 9.5 were fitted to the formula $\delta = (\delta^- + \delta^{2-} K_3/H^+)/(1 + K_3/H^+)$. The fit (*solid line*) furnished $K_3 = 1.97 \cdot 10^{-6} \pm 5.7 \cdot 10^{-8}$

by Metzler et al. (1973). In order to decide this question, we studied the titration curve of pyridoxamine phosphate with ^{31}P NMR spectroscopy (Fig. 2), and found that the second phosphate proton dissociates mainly at pK_3.

We use the simplest mechanism which is in agreement with all measurements discussed (Fig. 1). In the pH range between pK_2 and pK_4, the pH range of interest to us, this mechanism resembles that of 3-hydroxypyridine, except that the tautomeric equilibrium undergoes a change in overall charge at pK_3. We use the hypothesis that the dissociation of the second phosphate proton does no change the tautomeric equilibrium.

The relaxation spectrum of 3-hydroxypyridine has been studied in detail (Reiter et al. 1988). For pyridoxamine phosphate we expect to observe similar normal reactions: Between pK_2 and pK_4, the equilibration of neutral form and zwitterion, mode I, $\mathbf{A}_N = \mathbf{A}_Z$ ($\mathbf{A}_N^- = \mathbf{A}_Z^-$), should be important. Three pathways may contribute to this mode: direct intramolecular proton transfer; dissociative paths proceedings by simultaneous protonation and deprotonation of phenol group and ring nitrogen; and bimolecular reactions. (With bimolecular reactions we denote in this paper reactions which involve two molecules of the multibasic acid as reactants.) The second mode to be expected is more complicated and consists of two branches. The first branch, II a, is the overall reaction $\mathbf{A}^+ + x\,\mathbf{A}_N^- + (1-x)\,\mathbf{A}_Z^- = y\,\mathbf{A}_N + (2-y)\,\mathbf{A}_Z$, $0 \leqq x \leqq 1$,

$0 \leqq y \leqq 2$. It assumes its maximal amplitude at the isoelectric point between pK_2 and pK_3. Dissociative and biomolecular pathways contribute to this mode. The second branch, II b, the overall reaction $\mathbf{A}^{2-} + x\,\mathbf{A}_N + (1-x)\,\mathbf{A}_Z = y\,\mathbf{A}_N^- + (2-y)\,\mathbf{A}_Z^-$, $0 \leqq x \leqq 1$, $0 \leqq y \leqq 2$, is most prominent between pK_3 and pK_4. In addition, the proton dissociation equilibria at pK_2, pK_3 and pK_4 should play a role in the pH range of interest to us. We first compare our results with these idealized normal reactions and then discuss the actual simulated normal reactions.

Ultrasound absorption

We could detect excess ultrasound absorption between pH 3.5 and pH 5 and found a single relaxation process with maximal absorption at pH 4.5, at about the isoelectric point between pK_2 and pK_3. We measured this relaxation in the pH range just mentioned and for concentrations of pyridoxamine phosphate between about 0.05 and 0.15 mol l^{-1}. The inverse relaxation time can be described by the equation

$$\tau^{-1} = (2 \cdot 10^9 \pm 1.3 \cdot 10^8)(\mathbf{A}^+ + \mathbf{A}^-)\ s^{-1} + (3.1 \cdot 10^8 \pm 3.1 \cdot 10^7)(\mathbf{A}_N + \mathbf{A}_Z)\ s^{-1},$$

where the symbols of the species stand for the equilibrium concentrations, $\mathbf{A}^- = \mathbf{A}_N^- + \mathbf{A}_Z^-$ holds, and $pK_2 = 3.39$ and $pK_3 = 5.7$ were used to calculate the equilibrium concentrations. The data are plotted in Fig. 3 along with the relaxation spectrum, which we will discuss further below.

It is difficult to explain these results with mode I, the overall reaction $\mathbf{A}_N = \mathbf{A}_Z$. In the pH range considered here, there are two possible bimolecular reactions for this mode: $\mathbf{A}_N + \mathbf{A}^+ \rightleftharpoons \mathbf{A}_Z + \mathbf{A}^+$ and $2\,\mathbf{A}_N \rightleftharpoons 2\,\mathbf{A}_Z$. The rate constant of the first reaction has a diffusion controlled limit of $5 \cdot 10^8$ l mol^{-1} s^{-1}; a similar value has been determined for 3-hydroxypyridine. The second reaction involves a double proton transfer. For 3-hydroxypyridine, its rate constant was found to be about $2 \cdot 10^6$ l mol^{-1} s^{-1}. Using these values, the two reactions furnish the following contribution to the inverse relaxation time of mode I: $(5 \cdot 10^8 \cdot \mathbf{A}^+ + 2 \cdot 10^6 (\mathbf{A}_N + \mathbf{A}_Z))\ s^{-1}$. To explain our data, both rate constants would have to be significantly faster, especially the second. The term in the fit which is proportional to the concentration of $\mathbf{A}^-$ is difficult to explain with mode I. The only conceivable reaction contributing such a term is $\mathbf{A}_N + \mathbf{A}_Z^- \rightleftharpoons \mathbf{A}_Z + \mathbf{A}_N^-$. The diffusion controlled limit of its rate constant is about $5 \cdot 10^8$ l mol^{-1} s^{-1}. Since this reaction would take on its maximal amplitude at pK_3, where no excess ultrasound absorption has been observed, we can rule it out. The measured amplitude can also not adequately be described by mode I. A fit of the amplitude data to the normal reaction $\mathbf{A}_N = \mathbf{A}_Z$ furnishes: $pK_2 = 4$ and $pK_3 = 5.12$ (not shown).

Mode II a, the overall reaction $\mathbf{A}^+ + x\,\mathbf{A}_N^- + (1-x)\,\mathbf{A}_Z^- = y\,\mathbf{A}_N + (2-y)\,\mathbf{A}_Z$, $0 \leqq x \leqq 1$, $0 \leqq y \leqq 2$, is in better agreement with the inverse relaxation data than mode I. Four bimolecular reactions contribute to mode II a: $\mathbf{A}^+ + \mathbf{A}_N^- \rightleftharpoons \mathbf{A}_N + \mathbf{A}_Z$, $\mathbf{A}^+ + \mathbf{A}_N^- \rightleftharpoons 2\,\mathbf{A}_N$, $\mathbf{A}^+ + \mathbf{A}_Z^- \rightleftharpoons \mathbf{A}_N + \mathbf{A}_Z$ and $\mathbf{A}^+ + \mathbf{A}_Z^- \rightleftharpoons 2\,\mathbf{A}_Z$. The diffusion controlled limits for the rate constants of the four reactions are larger than 10^9 l mol^{-1} s^{-1} (Yiv et al. 1978). Taking the same forward rate constant k^{+-} for all four reactions, the coefficients in the normal reaction are calculated in the standard manner (Dubois and Dreyfus 1978; Reiter er al. 1988) as $x = 1/(1 + K_T)$ and $y = (3 + K_T)/(2(1 + K_T))$; we assumed that $K_T = K_T^-$ holds, vide supra. We then obtain for the inverse relaxation time:

$$(1/\tau)_{IIa} = 2\,k^{+-}(\mathbf{A}^+ + \mathbf{A}_N^- + \mathbf{A}_Z^-) + k^{+-} K_3/K_2\,(4 + (1 + 6\,K_T + K_T^2)/(2\,K_T))(\mathbf{A}_N + \mathbf{A}_Z).$$

Depending on the precise values of k^{+-}, pK_2 and pK_3, this expression can largely account for the measured inverse relaxation time. Fitting it to the data furnishes: $k^{+-} = 8.0 \cdot 10^8 \pm 5.4 \cdot 10^7\ s^{-1}$; $pK_2 = 3.79 \pm 0.06$; $pK_3 = 5.49 \pm 0.05$. With our data, K_T cannot be obtained from the fit; we have used $K_T = 9.3$. (With a large $K_T = 80$ we obtained $k^{+-} = 9.1 \cdot 10^8 \pm 6.6 \cdot 10^7\ s^{-1}$; $pK_2 = 3.58 \pm 0.05$; $pK_3 = 5.70 \pm 0.04$.) The Γ-factor of the amplitude of mode II a is

$$\Gamma_{IIa} = 1/(1/\mathbf{A}^+ + 1/(\mathbf{A}_N^- + \mathbf{A}_Z^-) + B/(\mathbf{A}_N + \mathbf{A}_Z))$$

$$B = (1 + 14\,K_T + K_T^2)/(4\,K_T)$$

In the pH range where the concentration of either $\mathbf{A}^+$ or $\mathbf{A}_N^- + \mathbf{A}_Z^-$ is smaller than the concentration of $\mathbf{A}_N + \mathbf{A}_Z$ divided by B, this amplitude falls off much faster than the measured amplitude. If the concentration of $\mathbf{A}_N + \mathbf{A}_Z$ determines the size of the amplitude, it falls off slower than the measured amplitude between pK_1 and pK_2; in this case the shape of the amplitude of mode II a is similar to the shape of the amplitude of mode I. By a proper choice of the constant B, the amplitude of mode II a can be brought into agreement with the measured amplitude. However, with the experimentally determined values for K_2 and K_3, K_T has to be increased significantly, i.e., to a value bigger than 100. With $K_T = 9.3$ the amplitude falls off faster from the isoelectric point than the measured amplitude, Fig. 3. If other overall neutral isomers with small equilibrium concentrations participated in the normal reaction with an appreciable stoichiometric coefficient, the shape of the amplitude would be more similar to the shape of the amplitude of mode I. The absolute size of the amplitude however would be smaller. In this work, we try to find a plausible explanation for the

Table 2. Proton transfer reactions of pyridoxamine phosphate

		K	k_f	k_r	ΔV	ΔH
$\mathbf{A}^+$	$\rightleftharpoons \mathbf{A}_N + H^+$	$4.24 \cdot 10^{-5}$	$8.47 \cdot 10^5$	$2.00 \cdot 10^{10}$	0.80	23.8
$\mathbf{A}^+$	$\rightleftharpoons \mathbf{A}_Z + H^+$	$3.94 \cdot 10^{-4}$	$7.88 \cdot 10^6$	$2.00 \cdot 10^{10}$	− 5.60	10.2
$\mathbf{A}_Z$	$\rightleftharpoons \mathbf{A}_Z^- + H^+$	$2.00 \cdot 10^{-6}$	$8.00 \cdot 10^4$	$4.00 \cdot 10^{10}$	−25.0	3.60
$\mathbf{A}_N$	$\rightleftharpoons \mathbf{A}_N^- + H^+$	$2.00 \cdot 10^{-6}$	$8.00 \cdot 10^4$	$4.00 \cdot 10^{10}$	−25.0	3.60
$\mathbf{A}^{2-} + H_2O$	$\rightleftharpoons \mathbf{A}_N^- + OH^-$	$6.21 \cdot 10^{-9}$	$6.22 \cdot 10^1$	$1.00 \cdot 10^{10}$	− 8.10	33.2
$\mathbf{A}_Z^- + H_2O$	$\rightleftharpoons \mathbf{A}_Z + OH^-$	$9.03 \cdot 10^{-11}$	1.81	$2.00 \cdot 10^{10}$	3.50	52.2
$\mathbf{A}_N$	$\rightleftharpoons \mathbf{A}_Z$	9.30	$1.40 \cdot 10^3$	$1.50 \cdot 10^2$	− 6.40	−13.6
$\mathbf{A}_N^-$	$\rightleftharpoons \mathbf{A}_Z^-$	9.30	$1.40 \cdot 10^3$	$1.50 \cdot 10^2$	− 6.40	−13.6
$\mathbf{A}^{2-} + H_2O$	$\rightleftharpoons \mathbf{A}_Z^- + OH^-$	$5.78 \cdot 10^{-8}$	$5.78 \cdot 10^2$	$1.00 \cdot 10^{10}$	−14.5	19.6
$\mathbf{A}_N^- + H_2O$	$\rightleftharpoons \mathbf{A}_N + OH^-$	$9.03 \cdot 10^{-11}$	1.81	$2.00 \cdot 10^{10}$	3.50	52.2
$\mathbf{A}_N^-$	$\rightleftharpoons H^+ + \mathbf{A}^{2-}$	$2.91 \cdot 10^{-8}$	$1.45 \cdot 10^3$	$5.00 \cdot 10^{10}$	−13.4	22.6
$\mathbf{A}_Z^-$	$\rightleftharpoons H^+ + \mathbf{A}^{2-}$	$3.12 \cdot 10^{-9}$	$1.56 \cdot 10^2$	$5.00 \cdot 10^{10}$	− 7.00	36.20
$\mathbf{A}^+ + \mathbf{A}_Z$	$\rightleftharpoons \mathbf{A}^+ + \mathbf{A}_N$	$1.07 \cdot 10^{-1}$	$5.37 \cdot 10^7$	$5.00 \cdot 10^8$	6.40	13.6
$\mathbf{A}_Z^- + \mathbf{A}^{2-}$	$\rightleftharpoons \mathbf{A}_N^- + \mathbf{A}^{2-}$	$1.07 \cdot 10^{-1}$	$2.15 \cdot 10^7$	$2.00 \cdot 10^8$	6.40	13.6
$2\mathbf{A}_Z$	$\rightleftharpoons \mathbf{A}^+ + \mathbf{A}_Z^-$	$5.08 \cdot 10^{-3}$	$5.08 \cdot 10^6$	$1.00 \cdot 10^9$	−19.4	− 6.60
$\mathbf{A}_N + \mathbf{A}_Z$	$\rightleftharpoons \mathbf{A}^+ + \mathbf{A}_Z^-$	$4.72 \cdot 10^{-2}$	$4.72 \cdot 10^7$	$1.00 \cdot 10^9$	−25.8	−20.2
$2\mathbf{A}_N$	$\rightleftharpoons \mathbf{A}^+ + \mathbf{A}_N^-$	$4.72 \cdot 10^{-2}$	$4.72 \cdot 10^7$	$1.00 \cdot 10^9$	−25.8	−20.2
$\mathbf{A}_N + \mathbf{A}_Z$	$\rightleftharpoons \mathbf{A}^+ + \mathbf{A}_N^-$	$5.08 \cdot 10^{-3}$	$5.08 \cdot 10^6$	$1.00 \cdot 10^9$	−19.4	− 6.60
$2\mathbf{A}_Z^-$	$\rightleftharpoons \mathbf{A}_Z + \mathbf{A}^{2-}$	$1.56 \cdot 10^{-3}$	$7.81 \cdot 10^5$	$5.00 \cdot 10^8$	18.0	32.6
$\mathbf{A}_N^- + \mathbf{A}_Z^-$	$\rightleftharpoons \mathbf{A}_Z + \mathbf{A}^{2-}$	$1.45 \cdot 10^{-2}$	$7.26 \cdot 10^6$	$5.00 \cdot 10^8$	11.6	19.0
$\mathbf{A}_N^- + \mathbf{A}_Z^-$	$\rightleftharpoons \mathbf{A}_N + \mathbf{A}^{2-}$	$1.56 \cdot 10^{-3}$	$7.81 \cdot 10^5$	$5.00 \cdot 10^8$	18.0	32.6
$2\mathbf{A}_N^-$	$\rightleftharpoons \mathbf{A}_N + \mathbf{A}^{2-}$	$1.45 \cdot 10^{-2}$	$7.26 \cdot 10^6$	$5.00 \cdot 10^8$	11.6	19.0
$\mathbf{A}_N + \mathbf{A}_Z^-$	$\rightleftharpoons \mathbf{A}_Z + \mathbf{A}_N^-$	1.00	$5.00 \cdot 10^8$	$5.00 \cdot 10^8$	0.00	0.00
H_2O	$\rightleftharpoons H^+ + OH^-$	$1.81 \cdot 10^{-16}$	$2.53 \cdot 10^{-5}$	$1.40 \cdot 10^{11}$	−21.5	55.8

Kinetic mechanism used for the simulation of the relaxation spectra in Figs. 3 and 4. Rate constants of intermolecular proton transfer in the thermodynamically favored direction are assumed to be diffusion controlled, see also text. The sum of the rate constants of the intramolecular proton transfer is set to a value which is to small to influence the results. The rate constants of the water dissociation are taken from the literature (Eigen 1963). The rate constants are given in standard units (l, mol, s). The reaction enthalpies and reaction volumes are taken from 3-hydroxypyridine (Reiter et al. 1988), phosphoric acid (Larson et al. 1982) and water (Christensen et al. 1976; Asano and Le Noble 1978) and are in units ml/mol and kJ/mol

experiments using all data available to us, but we do not attempt to achieve quantitative agreement between experiment and model by varying parameters arbitrarily.

With the equilibrium constants from Table 2, the Γ-factor of mode II a is about two times smaller than the Γ-factor of mode I. Consequently, in order for the two modes to be of comparable magnitude, the reaction volume of mode II a must be larger than the reaction volume of mode I. in Fig. 3, we show the simulated relaxation spectrum for an ultrasound experiment. We have included hydrolysis and protolysis reactions in the mechanism (Table 2), although only the bimolecular reactions involving two pyridoxamine phosphate species are important at the concentration of pyridoxamine phosphate used, i.e., ~ 0.1 mol l^{-1}. We have used reaction volumes determined for 3-hydroxypyridine (Reiter et al. 1988) and phosphoric acid (Larson et al. 1982). With these data, the amplitude of mode II a is indeed much larger than the amplitude of mode I because of the large reaction volume of the second dissociation of phosphoric acid. However, as already noted, the amplitude of mode II a cannot explain the measured amplitude fully. It is possible that the measured signal is an average of mode II a and mode I. At the isoelectric point, mode II a would prevail. At lower pH, mode I would participate. At higher pH, only mode II would contribute to the overall effect because mode I is too slow. We have indeed noted that the data near pH 5 are more uncertain than the data at lower pH. The peaks are also broader at pH 5. The rate constants of the bimolecular reactions of mode I, i.e., in particular the rate constant of the reaction $\mathbf{A}_N + \mathbf{A}^+ \rightleftharpoons \mathbf{A}_Z + \mathbf{A}^+$, would have to be larger than observed for 3-hydroxypyridine to make this explanation acceptable. The precise value required depends on K_2, see also Fig. 3. The amplitude of mode I would also have to be larger than in the simulation in Fig. 3.

We found no appreciable ultrasound absorption at the isoelectric point between pK_3 and pK_4. In principle, similar proton transfer reactions should occur as at the isoelectric point between pK_2 and pK_3, i.e., mode I, here mainly $\mathbf{A}_N^- = \mathbf{A}_Z^-$, and mode II b. All bimolecular reactions are expected to be slower because of the more unfavorable charges of the reacting molecules. With our equipment, we can detect ultrasound absorption for relaxation times faster than $5 \cdot 10^6$ s^{-1}. Even with low estimates for the bimolecu-

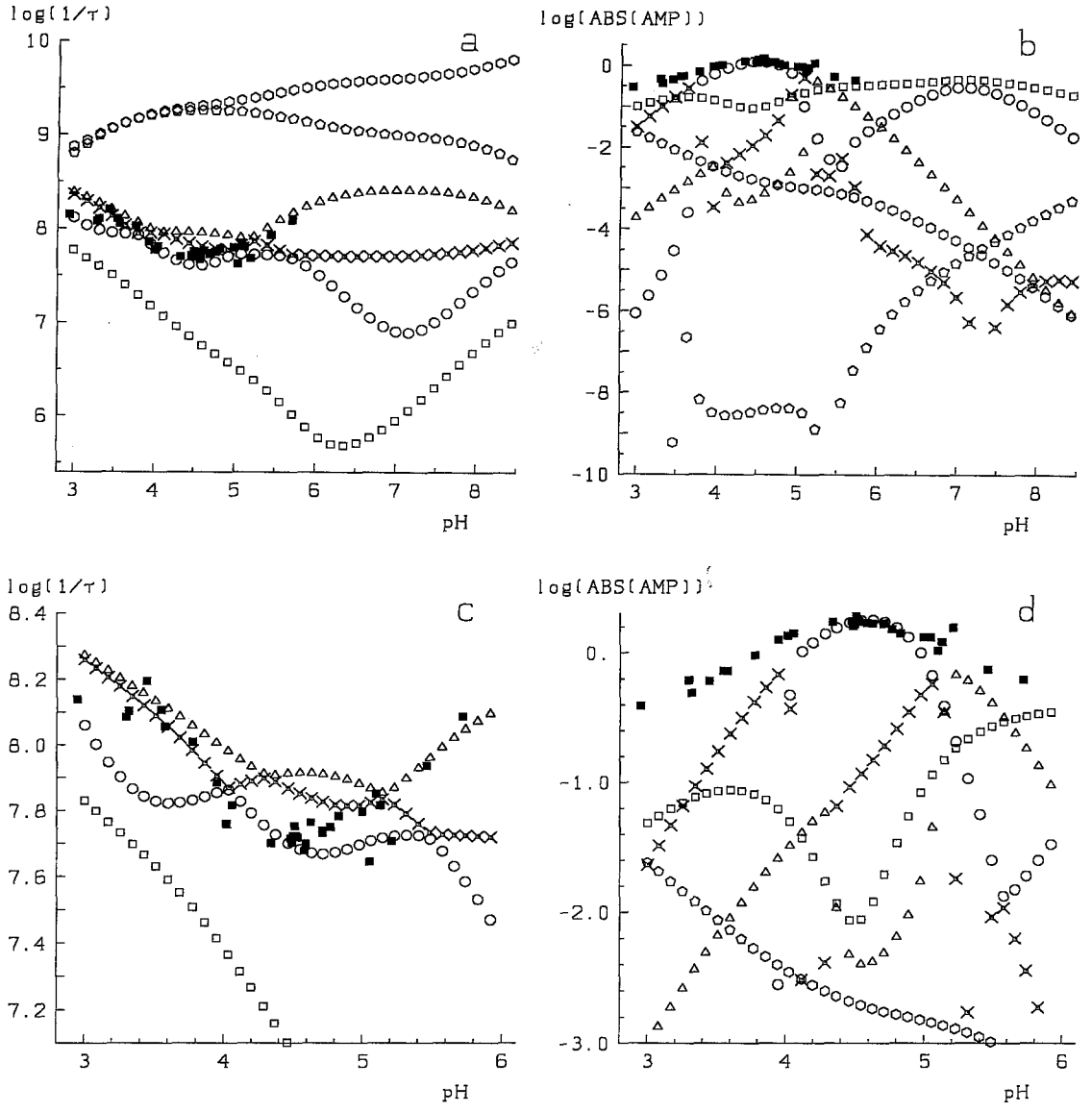

Fig. 3 a–d. Relaxation spectrum simulated for an ultrasound experiment. The total concentration of pyridoxamine phosphate is 0.1 mol l^{-1}. *Open squares*: mode I; *circles* between pH 6 and pH 8: mode II b. *Triangles* between pH 5.4 and pH 6, *circles* between pH 4.2 and pH 5.0 and *crosses* between pH 3 and pH 4: mode II a. See also Table 3. The experimental data (*full squares*) have been corrected to the concentration used in the plot with the expressions obtained from the fits, see text for these expressions, and are shown as small dark squares. **a, b** $pK_2 = 3.36$, $pK_3 = 5.7$, $k^{+-} = 1.35 \cdot 10^9$; **c, d** $pK_2 = 3.75$, $pK_3 = 5.55$, $k^{+-} = 8.2 \cdot 10^8$. Other parameters are as in Table 2. The relaxation times are in units s and the amplitudes, $\Gamma \Delta V_S^2$, are in units ml/(1000 mol). The calculated maximal amplitude of mode II a is 1.26 ml/(1000 mol) in **b** and 1.79 ml/(1000 mol) in **d**. The measured amplitude reaches a maximum of about 1.63 ml/(1000 mol) at the same concentration of pyridoxamine phosphate as used in the plot (0.1 mol l^{-1}). To facilitate the comparison, we have adjusted the measured amplitude to the amplitude of mode II a in **b** and **d**

lar rate constants of mode II b we would, therefore, still expect to detect absorption. However, mode I is most likely already too slow to be detected. Because the difference between pK_3 and pK_4 is larger than the difference between pK_2 and pK_3, the Γ-factor of mode II b is smaller than the Γ-factor of mode II a. With the reaction volumes of 3-hydroxypyridine and phosphoric acid, we indeed calculate a significantly smaller amplitude for mode II b than for mode II a (Figs. 3 a and b).

The simulated normal reactions in Fig. 3 are more complicated than the idealized modes I and II, but the conclusions reached so far remain correct. Near the isoelectric point between pK_2 and pK_3, actual mode I comprises a significant amount of mode II a, although with different stoichiometric coefficients. This is also discernible from the amplitude, which assumes a local minimum at that pH, in contrast to the amplitude of idealized mode I. It is clear that mode I cannot explain our measurements. The relaxation time of mode II a

Table 3. Normal reactions calculated for an ultrasound experiment

pH = 4.44	A^+	A_N	A_Z	A_N^-	A_Z^-	A^{2-}	H^+	OH^-	H_2O	
I	0.120	0.759	−1.000	0.060	0.061	0.000	0.001	0.000	0.000	$4.12 \cdot 10^{-1}$
II a	−0.707	0.418	1.000	−0.027	−0.684	0.000	−0.003	0.000	0.000	1.00
	−0.159	1.000	−0.682	−0.812	0.655	−0.001	−0.001	0.000	0.000	$3.38 \cdot 10^{-2}$
	−0.467	1.000	0.426	−0.939	−0.507	0.488	−0.003	0.000	0.000	$3.69 \cdot 10^{-4}$
	0.017	0.099	0.869	−0.092	−0.864	−0.028	−0.029	1.000	−1.000	$1.22 \cdot 10^{-8}$
	0.907	−0.082	−0.733	−0.009	−0.084	0.000	−1.000	0.000	0.000	$3.19 \cdot 10^{-3}$

Changes in concentration of the species of pyridoxamine phosphate and water are tabulated for the six normal reactions of the simulation of Figures 3 a and 3 b. The normal reactions appear in the order of their relaxation time; the slowest reaction is listed first. In each normal reaction, the species with the biggest change is normalized to plus or minus unity. The relative magnitude of each normal mode is given in the last column

can approximately describe the measured relaxation time. The appropriate value for k^{+-} varies from $8 \cdot 10^8$ l mol^{-1} s^{-1} to $1.4 \cdot 10^9$ l mol^{-1} s^{-1}, depending on the precise values of pK_2 and pK_3 used. Figures 3 c and d show the range around pH 4.5 more closely. there are two further modes near mode II a. At the isoelectric point mode II a is the slowest, at pH 5.5 it is the fastest, and at pH 3.6 it is the second fastest of these three modes. At the isoelectric point, mode II a has a small amount of (idealized) mode I mixed in. The next faster relaxation consists also of mode II a, although with different stoichiometric coefficients, and comprises also the reaction $\mathbf{A}_N + \mathbf{A}_Z^- \rightleftharpoons \mathbf{A}_Z + \mathbf{A}_N^-$. The amplitude of this relaxation is about one tenth of the amplitude of mode II a. The next faster relaxation comprises reactions of mode II a and II b; its amplitude is negligible. Mode II a is discontinuous between pH 4.5 and 5.2, i.e., the relaxations exchange amplitudes in that range.

Based on results obtained for 3-hydroxypyridine (Schuster et al. 1976) and o-amino-benzoic acid (Reiter et al. 1988) and based on our simulations, we have so far assumed that the ultrasound absorption is caused by proton transfer reactions. However, in aqueous solutions of some aromatic compounds, stacking has been identified as the process responsible for ultrasound absorption. Pörschke and Eggers (1972) have measured the aggregation of an uncharged adenine derivative and found a diffusion controlled aggregation constant of 10^9 l mol s^{-1}. We have observed maximal ultrasound absorption at a pH where pyridoxamine phosphate is uncharged. But it is highly polar – $\mathbf{A}_Z$ has four local charges – which should reduce the probability of stacking in water. The amplitude of the aggregation of the overall neutral form has a similar pH dependence as mode I, and therefore the measured amplitude could be simulated by an average of mode II a and aggregation. However, other observations are not in agreement with an aggregation process: The amplitude of mode II a depends linearly on the concentration of pyridoxamine phosphate, while the amplitude of an aggregation model depends non-linearly on the concentration of pyridoxamine phosphate. In Fig. 3, we plotted the quotient of amplitude and concentration, i.e., the measured amplitudes are scaled to a concentration of 0.1 mol l^{-1}. Although this quotient shows a slight upward trend with increasing concentration of pyridoxamine phosphate (that trend is not shown, only the scatter of the quotient), this variation is small and within the error of the measurement (Fig. 3). In addition, the relaxation time calculated for an aggregation model should contain a large constant term (Pörschke and Eggers 1972), which we did not observe. Literature data do not support an aggregation model either: Morozov et al. (1966) have studied the Beer law for all forms of pyridoxamine phosphate in the concentration range of 10^{-5} to 10^{-2} mol l^{-1} and found no indication for aggregation. Our measurements were done at a higher concentration, at about 0.1 mol l^{-1}, however. Jaworski and O'Leary (1979) reviewed ^{13}C NMR spectra of pyridoxamine phosphate and showed a diagram of the chemical shifts of all carbons of pyridoxamine phosphate at a concentration of 0.1 mol l^{-1} with changing pH, including a data point at pH 4.5, but no anomalous chemicals shifts were found at pH 4.5. With the stacking model, it is easy to explain the absence of ultrasound absorption at the isoelectric point between pK_3 and pK_4 because no aggregation of the negatively charged molecules $\mathbf{A}_N^-$ and $\mathbf{A}_Z^-$ is expected.

Yiv et al. (1978) measured the ultrasound absorption of aqueous solutions of cytidine 5'-phosphate and other nucleotide phosphates. They attributed the absorption to a reaction which is essentially a simpler version of our mode II and reported a rate constant of $1.9 \cdot 10^9$ l mol^{-1} s^{-1} (k^{+-}) and a reaction volume of −23.8 ml/mol. They concluded that mode II is modified by a fast aggregation of the overall neutral form in some nucleotide phosphates, but that this aggregation is not directly observed in the ultrasound absorption. For simplicity we assume that neutral form and zwitterion dimerize with equilibrium constant K and that they are indistinguishable in the dimerization. By further assuming that the dimerizations is fast, the nor-

Table 4. Normal reactions calculated for a temperature jump experiment. Changes in concentration for the six normal reactions of the simulation of Fig. 4c; analogous to Table 3

	$\mathbf{A}^+$	$\mathbf{A}_N$	$\mathbf{A}_Z$	$\mathbf{A}_N^-$	$\mathbf{A}_Z^-$	$\mathbf{A}^{2-}$	H^+	OH^-	H_2O	
pH = 7.16										
I	0.000	0.038	0.035	0.854	−1.000	0.073	0.001	0.001	−0.001	1.000
II b	0.000	0.057	0.660	−0.431	−1.000	0.714	0.004	0.009	−0.009	$3.85 \cdot 10^{-1}$
	0.000	0.976	−0.961	−1.000	0.971	0.015	0.000	0.000	0.000	$3.09 \cdot 10^{-4}$
	0.000	0.006	0.056	0.087	0.789	−0.938	0.000	1.000	−1.000	$7.43 \cdot 10^{-3}$
	0.279	−0.116	−1.000	0.041	0.715	0.081	0.640	0.001	−0.001	$8.60 \cdot 10^{-5}$
	−0.051	−0.078	−0.732	0.040	0.734	0.086	1.000	0.002	−0.002	$8.86 \cdot 10^{-4}$
pH = 5.72										
I	0.001	0.822	−0.818	0.989	−1.000	0.006	0.001	0.000	0.000	1.000
	0.000	0.937	−1.000	−0.785	0.908	−0.061	0.000	0.000	0.000	$2.13 \cdot 10^{-3}$
II b	0.004	0.897	−0.475	−1.000	0.143	0.431	0.004	0.003	−0.003	$6.85 \cdot 10^{-2}$
	−0.302	0.118	1.000	−0.078	−0.735	−0.003	−0.517	0.000	0.000	$1.02 \cdot 10^{-2}$
	0.061	0.041	0.403	−0.005	−0.149	−0.351	0.084	1.000	−1.000	$1.09 \cdot 10^{-3}$
	−0.576	0.020	0.133	0.040	0.381	0.001	1.000	0.000	0.000	$4.02 \cdot 10^{-2}$
pH = 4.44										
I	0.004	0.988	−1.000	0.095	−0.086	0.000	0.005	0.000	0.000	1.000
	0.017	0.935	−1.000	−0.541	0.590	0.000	0.030	0.000	0.000	$6\,54 \cdot 10^{-2}$
II a	−0.296	0.137	1.000	−0.088	−0.753	0.000	−0.544	0.000	0.000	$3.35 \cdot 10^{-2}$
	0.189	0.430	0.114	−0.865	−0.868	1.000	0.083	0.005	−0.005	$9.84 \cdot 10^{-5}$
	0.584	0.001	0.008	−0.051	−0.519	−0.022	−0.198	1.000	−1.000	$4.27 \cdot 10^{-5}$
	−0.965	0.091	0.838	0.003	0.032	0.000	1.000	0.000	0.000	$5.13 \cdot 10^{-1}$

mal reaction can be calculated (Bernasconi 1976): The stoichiometric coefficients of $\mathbf{A}_N$ and $\mathbf{A}_Z$ in the normal reaction II a are additionally divided $1 + 4\,K\,(\mathbf{A}_N + \mathbf{A}_Z)$ and the sum of all dimer species has a stoichiometric coefficient of $8\,K\,(1 + K_T)(\mathbf{A}_N + \mathbf{A}_Z)$ divided by the same denominator as the coefficients of $\mathbf{A}_N$ and $\mathbf{A}_Z$. The inverse relaxation time is the same as already given, but the term proportional to the equilibrium concentration of $\mathbf{A}_N + \mathbf{A}_Z$ is divided by $1 + 4\,K\,(\mathbf{A}_N + \mathbf{A}_Z)$. The Γ-factor calculated for the present model is the same as that given above for mode II a, but the constant B is different:

$$B_1 = (1 + 14\,K_T + K_T^2 + 2\,K\,(\mathbf{A}_N + \mathbf{A}_Z)(1 + 30\,K_T + K_T^2))/(4\,K_T(1 + 4\,K\,(\mathbf{A}_N + \mathbf{A}_Z))^2).$$

The shape of the amplitude as a function of pH for the model with aggregation differs from that of mode II a for three reasons: First, B_1 is smaller than B, making the shape of the amplitude even less satisfactory than that of mode II a, vide supra. Second, the equilibrium concentrations of $\mathbf{A}^+$ and $\mathbf{A}^-$ vary differently with pH in the present model than in the proton transfer model without dimerization because of the dimer, i.e., the concentration ratio of for instance $\mathbf{A}^+$ at pK_2 and at the isoelectric point is larger by at most a factor of two for the present model than for the model without aggregation, making the shape of the amplitude broader as a function of pH. However, a factor of two is clearly not enough (Fig. 3). Third, the reaction volume at constant entropy of the present model calculates as

$$(\Delta V_S)_{\text{II a + Dim.}} = (\Delta V_S)_{\text{II a}} + 4\,(\Delta V_S)_{\text{Dim.}}\,K\,(\mathbf{A}_N + \mathbf{A}_Z)/(1 + 4\,K\,(\mathbf{A}_N + \mathbf{A}_Z)),$$

where Dim. stands for the dimerization reaction $\mathbf{A}_N\,(\mathbf{A}_Z) + \mathbf{A}_N\,(\mathbf{A}_Z) \leftrightharpoons D$. Since the concentration of $\mathbf{A}_N + \mathbf{A}_Z$ changes at most by a factor of two between pK_1 and pK_2 and the reaction volume of the dimerization step is smaller in absolute value than the reaction volume of mode II a (Yiv et al. 1978; Pörschke and Eggers 1972), the change of the reaction volume of the present model with pH between pK_1 and pK_2 is not very significant. Therefore, to assume a fast dimerization step does not bring about a significantly better agreement between model and experiment.

Temperature jump experiments

We did temperature jump experiments in the range of pH 3 to pH 9 and for concentrations of pyridoxamine phosphate between $2 \cdot 10^{-4}$ and $8 \cdot 10^{-4}$ mol l^{-1} and found essentially one relaxation. The inverse relaxation time shows the typical pH profile of proton transfer reactions (Fig. 4). The data show too much scatter to allow a reliable determination of the concentration dependence of the inverse relaxation time. Qualitatively it is clear that the inverse relaxation time

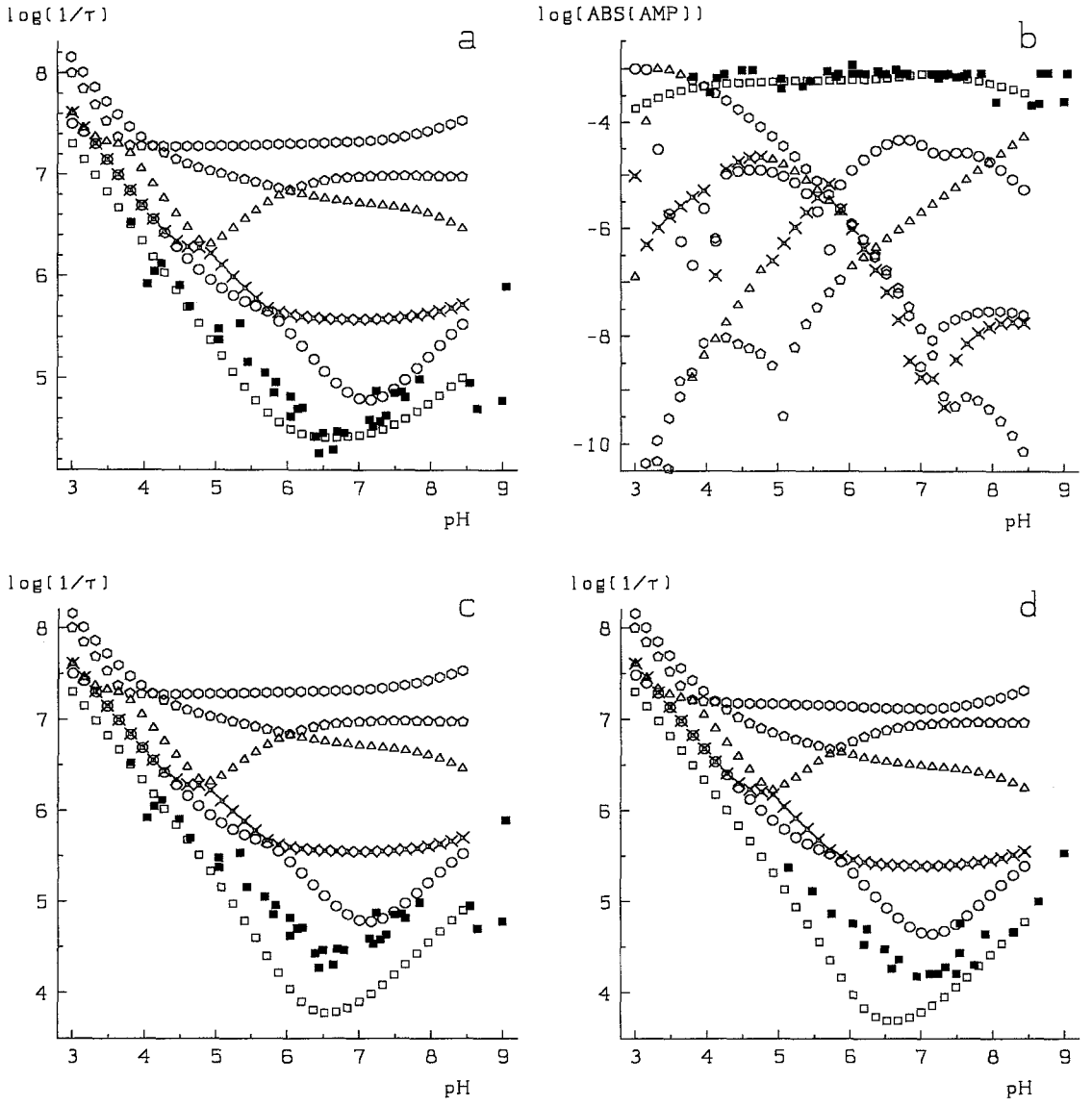

Fig. 4 a–d. Relaxation spectrum simulated for a temperature jump experiment. *Open squares*: mode I. *Circles* between pH 6 and pH 8.5: mode II b. See also Table 4. The data are shown as *full squares*. **a, b** $k_{43} = k_{65} = 2 \cdot 10^4\ s^{-1}$. The total concentration of pyridoxamine phosphate is 0.0005 mol l^{-1} in **a, b, c** and 0.0003 mol l^{-1} in **d**. Other parameters are as in Table 2. The amplitudes are given as extinction and are arbitrarily scaled. We have used an extinction coefficient of 1 for $\mathbf{A}_Z$ and $\mathbf{A}_Z^-$ and an extinction coefficient of 0 for all other species. The amplitude data have been adjusted to coincide with the simulated amplitude of mode I in **b**

between pH 7 and pH 8 does depend on the concentration of pyridoxamine phosphate. Between pH 5.5 and pH 7, the data seem to be almost independent of the concentration of pyridoxamine phosphate, however. At pH 8, we observed a second faster relaxation, but could not measure it accurately. We have simulated the relaxation spectrum for two concentrations of pyridoxamine phosphate, Fig. 4. It is likely that the observed relaxation is due to mode I. However, the measured relaxation time is faster than the simulated relaxation time. Even if we increase the rate constants of the bimolecular and dissociative pathways slightly above the diffusion controlled limits, this discrepancy remains (not shown). There are three explanations for this difference. First, the intramolecular proton transfer rate constant has to be set to about $2 \cdot 10^4\ s^{-1}$ in the thermodynamically preferred direction (Fig. 4 a). Although the relaxation time at the minimum is better simulated, the acid and basic branches are still not satisfactory. Second, the bimolecular reaction $\mathbf{A}_N + \mathbf{A}_Z^- = \mathbf{A}_Z + \mathbf{A}_N^-$ and analogous paths via dissociative reactions are faster than the overall relaxation $\mathbf{A}_N = \mathbf{A}_Z (\mathbf{A}_N^- = \mathbf{A}_Z^-)$. However, we did not observe a change in the sign of the amplitude at $pH = pK_3$ and

found no significant concentration dependence of the inverse relaxation time at pK_3. See also the discussion of the relaxation spectrum below. Third, our measurements may be averages of mode I and mode II. Mode II is always faster than mode I and contributes the most at the isoelectric points. When the second mode is considerably faster than the first mode, its relative contribution is smaller, keeping the overall effect about the same.

Since it is not possible with our data to establish the rate constant of the intramolecular proton transfer reaction, we take a conservative view and assume that our results are an average of mode II and mode I. Again, we merely suggest that result, but do not calculate the average because it depends on parameters, i.e., reaction enthalpies and rate constants, for which we know only approximate values.

In the simulation in Fig. 4, mode I is the slowest relaxation, and between pH 4.5 and pH 8, it has the largest amplitude. Actual simulated mode I is almost entirely the reaction $\mathbf{A}_N = \mathbf{A}_Z$ ($\mathbf{A}_N^- = \mathbf{A}_Z^-$) (Table 4). Between pH 6 and pH 8, mode II b is the second slowest relaxation and has the second largest amplitude. It is well described by idealized mode II b. Above pH 8, the hydrolysis reactions of the proton dissociation equilibrium at pK_4 become important. At the isoelectric point between pK_2 and pK_3, actual mode II a comprises also the reaction $\mathbf{A}_N + \mathbf{A}_Z^- \rightleftharpoons \mathbf{A}_Z + \mathbf{A}_N^-$. This reaction relaxes back in the next slower relaxation. At lower pH, the protolysis reactions of the proton dissociation equilibrium at pK_2 become prominent.

Conclusion and discussion

Near the isoelectric point of many dibasic acids two normal reactions may be observed: Mode I, the equilibration of neutral form and zwitterion, $\mathbf{A}_N = \mathbf{A}_Z$, and mode II, the overall reaction $\mathbf{A}^+ + \mathbf{A}^- = x\,\mathbf{A}_N + (2-x)\,\mathbf{A}_Z$, $0 \leqq x \leqq 2$. Pyridoxamine phosphate is a pentabasic acid. We assumed that at pK_1 the first phosphate proton dissociates and that at pK_5 the amino proton dissociates. The latter assumption is based on ^{13}C NMR data (Jaworsky and O'Leary 1979). Therefore, in the range between pH 3 and pH 8, pyridoxamine phosphate can be considered a tribasic acid. Using UV-visible absorption data from the literature and our ^{31}P NMR measurements, we can further assume that the second of these three protons, the second phosphate proton, dissociates without affecting the thermodynamic equilibrium between neutral form and zwitterion. We then find that between pK_2 and pK_4 two modes are of significance: mode I, the equilibration between neutral form and zwitterion, $\mathbf{A}_N(\mathbf{A}_N^-) = \mathbf{A}_Z(\mathbf{A}_Z^-)$, and mode II which consists of two branches:

$$\text{II a:}\quad \mathbf{A}^+ + x\,\mathbf{A}_N^- + (1-x)\,\mathbf{A}_Z^- = y\,\mathbf{A}_N + (2-y)\,\mathbf{A}_Z,\quad 0 \leqq x \leqq 1,\ 0 \leqq y \leqq 2;$$

$$\text{II b:}\quad \mathbf{A}^{2-} + x\,\mathbf{A}_N + (1-x)\,\mathbf{A}_Z = y\,\mathbf{A}_N^- + (2-y)\,\mathbf{A}_Z^-,\quad 0 \leqq x \leqq 1,\ 0 \leqq y \leqq 2;$$

the coefficients x and y are different in the two branches; they depend on the rate constants of all reactions involved in the mode.

If more ionic forms of pyridoxamine phosphate are considered, the two modes are more general. Mode I is then the equilibration of tautomeric equilibria, i.e., the equilibration of species with the same overall charge, and mode II is the overall reaction $2\,\mathbf{A}^n = \mathbf{A}^{n+1} + \mathbf{A}^{n-1}$. The latter consists of several branches with different charges n, and the individual ionic forms with a given overall charge have stoichiometric coefficients determined by their kinetic contributions to the normal reaction. The concentration and pH dependence of these general modes is similar to the concentration and pH dependence of the idealized modes I and II written above, and, therefore, our general conclusions about the modes are unaffected by the simplifying assumptions made.

We measured ultrasound absorption at the isoelectric point between pK_2 and pK_3 and found that the inverse relaxation time can approximately be simulated by mode II a. The amplitude of this mode falls off faster from the isoelectric point with changing pH than the measured data, however. Tentatively we explained the data by an average of mode II a and mode I. For the bimolecular reactions of mode I we would have to assume rate constants which are larger than found for 3-hydroxypyridine. Since the amplitude of the aggregation of the overall neutral form has a similar pH dependence as ther amplitude of mode I, the amplitude data could also be explained by an average of mode II a and aggregation. However, the measured relaxation time is not in agreement with an aggregation model. In addition, published UV-visible data and ^{13}C NMR data do not indicate aggregation of pyridoxamine phosphate. To include a fast dimerization step of the overall neutral form into the mechanism, as proposed by Yiv et al. (1978) for nucleotide phosphates, does not improve the agreement between model and data.

We did temperature jump experiments between pH 3 and pH 9 and for concentrations of pyridoxamine phosphate between $2 \cdot 10^{-4}$ and $8 \cdot 10^{-4}$ mol l^{-1}. The relaxation is best explained by mode I. To get better quantitative agreement experiment and simulation, either an intramolecular rate constant of about $2.0 \cdot 10^4\ s^{-1}$ has to be assumed or the observed relaxation has to be taken as an average of mode I and mode II.

We have used the reaction volumes and reaction enthalpies of 3-hydroxypyridine and phosphoric acid for our simulation. The reaction volume of the second proton dissociation of phosphoric acid is large, about −25 ml/mol, which explains why mode II has a larger amplitude than mode I in the ultrasound experiment. On the other hand, the reaction enthalpy of the second dissociation of phosphoric acid is comparably small, which explains why mode I has a larger amplitude than mode II in the temperature jump experiment.

Acknowledgements. The work in Vienna has been supported financially by the Austrian "Fonds zur Förderung der wissenschaftlichen Forschung" (Projekt Nr. 2015 and 3388). Johannes Reiter received a stipend from the Max-Planck-Gesellschaft to visit the Max-Planck-Institut in Göttingen, FRG. He thanks the group of Professor M. Eigen for their hospitality and their support. Dr. H. H. Füldner helped us with the NMR measurements, Herr Richmann helped us with the ultrasound experiments and the computer staff of the group of Professor L. De Maeyer helped us with data transfer and computations.

References

Anderson FJ, Martell AE (1964) Pyridoxal phosphate: molecular species in solution. J Am Chem Soc 86:715–720

Asano T, Le Noble WJ (1978) Activation and reaction volumes in solution. Chem Rev 78:407–490

Bernasconi CF (1976) Relaxation kinetics. Academic Press, New York, pp 99–102

Bernasconi CF (ed) (1986) Techniques of chemistry, vol 6. John Wiley, New York, Part I and II

Christensen JJ, Hansen LD, Izatt RM (1976) Handbook of proton ionization heats. John Wiley, New York

Dubois JE, Dreyfus, ME (1978) Dynamic studies by chemical relaxation of prototropic equilibria in solution: recent advances. In: Laszlo P (ed) Protons and ions involved in fast dynamical phenomena. Elsevier, Amsterdam, pp 169–190

Eggers F (1967/1968) Eine Resonatormethode zur Bestimmung von Schallgeschwindigkeit und Dämpfung in geringen Flüssigkeitsmengen. Acustica 19:323–329

Eggers F, Funck T (1973) Ultrasonic measurements with milliliter liquid samples in the 0.5–100 MHz range. Rev Sci Instrum 44:969–977

Eigen M (1963) Protonenübertragung, Säure-Base-Katalyse und enzymatische Hydrolyse. Teil I: Elementarvorgänge. Angew Chem 75:489–508

Eigen M, DeMaeyer L (1974) Theoretical basis of relaxation spectrometry. In: Hammes GG (ed) Techniques of chemistry, vol 6, part II. John Wiley, New York, pp 63–146

Feldmann K, Gaugler BJM, Winkler H, Helmreich EJM (1975) Conformational transitions in glycogen phosphorylase reported by covalently bound pyridoxamine derivatives. Biochemistry 13:2222–2230

Hoffmann GW (1972) Entwicklung einer schnellen Temperatur-Sprung-Anlage und ihre Anwendung auf kooperative Basenpaarung. Dissertation, Universität Braunschweig

Jaworsky RJ, O'Leary MH (1979) ^{13}C NMR spectroscopy of the vitamin B_6 group. Methods Enzymol 62:436–454

Larson JW, Zeeb KG, Loren GL (1982) Heat capacities and volumes of dissociation of phosphoric acid (1st, 2nd, and 3rd), bicarbonate ion, and bisulfate ion in aqueous solution. Can J Chem 60:2141–2150

Metzler DE, Harris CM, Johnson RJ, Siano DB, Thomson JA (1973) Spectra of 3-hydroxypyridines. Band-shape analysis and evaluation of tautomeric equilibria. Biochemistry 12: 5377–5392

Morozov YV, Bazhulina NP, Karpeiskii MY, Ivanov VI, Kuklin AI (1966) Optical and luminescent properties of vitamin B_6 and its derivatives. III. Pyridoxamine and pyridoxamine-5′-phosphate. Biofizika 11:228–236

Pörschke D (1976) Cable temperature jump apparatus with improved sensitivity and time resolution. Rev Sci Instrum 47: 1363–1369

Pörschke D, Eggers F (1972) Thermodynamics and kinetics of base-stacking interactions. Europ J Biochem 26:490–498

Reiber H (1972) Photochemical reactions of vitamin B_6 compounds, isolation and properties of products. Biochim Biophys Acta 279:310–315

Reiter J, Beyer A, Potschka M, Schuster P, Winkler H, Ebeling H, Franck EU (1988) Proton transfer reactions of dibasic acids in aqueous solution: 3-hydroxypyridine and anthranilic acid. J Phys Chem (in press)

Schuster P, Tortschanoff K, Winkler H (1976) Protonenübertragungsreaktionen zweibasischer Säuren in wäßriger Lösung: 3-Hydroxypyridin. Z Naturforsch 31c:219–224

Schuster P, Wohlschann P, Tortschanoff K (1977) Dynamics of proton transfer in solution. In: Pecht I, Rigler R (eds) Chemical relaxation in molecular biology. Springer, Berlin Heidelberg New York, pp 107–190

Williams VR, Neilands JB (1954) Apparent ionization constants, spectral properties and metal chelation of the cotransaminases and related compounds. Arch Biochem Biophys 53:56–70

Yiv S, Lang J, Zana R (1978) Ultrasonic absorption in aqueous solutions of nucleotides and nucleosides. III. Kinetics of proton exchange in cytidine 5′-monophosphate and xanthosine 5′-monophosphate. In: Laszlo P (ed) Protons and ions involved in fast dynamical phenomena. Elsevier, Amsterdam, pp 311–322